Composites Part B: Engineering, 95:40—47 (2016)

INFLUENCE OF PLY CLUSTER THICKNESS AND LOCATION ON MATRIX CRACKING EVOLUTION IN OPEN-HOLE COMPOSITE LAMINATES

M. M. Moure[a], S. K. García-Castillo[a], S. Sánchez-Sáez[a], E. Barbero[a*], E. J. Barbero[b]

[a] Department of Continuum Mechanics and Structural Analysis, University Carlos III of Madrid, Avda de la Universidad 30, 28911 Leganés, Madrid, Spain

[b] Mechanical and Aerospace Engineering, West Virginia University, Morgantown, WV 26506, USA

Keywords: B. Stress concentration; B. Strength; C. Damage Mechanics; C. Numerical analysis; Open-hole composite laminates

Abstract

The influence of cluster thickness and its position on the damage evolution of open-hole composite laminates, subjected to uniaxial in-plane tensile loads, is studied in this work. The Discrete Damage Mechanics model of Barbero-Cortes augmented by a fiber damage criterion is employed. Several stacking sequences with clusters in different positions and thicknesses inside the laminate are analyzed. The influence of cluster thickness and its location on: the crack-density evolution, applied load, longitudinal stress and its contour plots is studied for all the stacking sequences selected.

1. Introduction

Many composite structures, such as aircraft frames, contain thousands of holes for joining purposes and open cut-outs for access. An open hole on a composite structure produces a stress gradient that increases the stress field in its proximity. Laminate damage usually appears at points of stress concentration. The strength, the stiffness and the service life of a notched structure, suffer a considerable reduction compared with the un-notched structure. Hence, the study of the influence of a hole on composite structures is an important task for a successful design.

The estimation of open-hole laminate strength is a very complicated problem, even under simple load cases [1], due to the interaction of various modes of damage, such as matrix cracking, delamination, and fiber failure, which produce a loss of load carrying capacity and/or loss of integrity if they appear simultaneously. This strength is dependent on a number of variables such as material properties, specimen size, hole diameter, stacking sequence, laminate lay-up, etc.

Generally, it is established that the strength decreases with increasing size of specimens with constant width-to-diameter ratio [2]. Recent studies shed new light into damage mechanics behind the size effect. Camanho et al. [3] carried out an experimental program to validate a damage model. From experimental results they observed that, an increase in the hole diameter of specimens with constant width/diameter, results in strength

reduction. This effect was caused by the development of a fracture process zone. For small specimens, this zone extended towards the edges of the specimen and the average stress at the fracture plane tends to the un-notched strength of the laminate. Erçin et al. [4] compare the size effect of notched composite laminates loaded under tension and compression. Also, they identified the failure mechanism sequence on the outer ply of the composite laminate.

The effect of using different stacking sequences in open-hole laminates is reflected by a modification in the strength and the failure modes of them. Usually, the most commonly used laminates lay-ups are a combination of 0º, 90º or ±45º angles. Since ply thickness of pre-preg is constant, when a thicker laminate is needed, it is expedient to cluster multiple plies with the same orientation (called ply-level scaling). Although this option could be advantageous due to its simplicity and readiness, it may be inefficient in terms of structural behavior [5]. The use of clusters of plies in a laminate increases the effective thickness of each ply-orientation. Another option to increase the thickness of the laminate is to increase the number of sublaminates with the same laminate stacking sequence (LSS) as the original laminate. Increasing the thickness of a laminate by adding sublaminates is called "sublaminate level scaling", whereas increasing the thickness of the laminates by clustering is called "ply-level scaling" or "clustering".

Harris and Morris [6] suggested that the open-hole strength decreases with number of sublaminates in quasi-isotropic lay-ups. The higher the number of sublaminates, the more confined is the damage to a zone close to the surface of the laminate, and thus less stress redistribution appears in the laminate. Furthermore, Vaidya et al. [7] analyzed notch strength behavior of cross-ply and quasi-isotropic laminates as a function of ply thickness resulting from clustering. They found that, as far as notch strength is concerned, ply thickness has more effect on cross-ply laminates than quasi-isotropic laminates.

Green et al. [8] studied the effect of laminate thickness, ply thickness, and hole diameter on the open-hole tensile strength of quasi-isotropic composite laminates. For both cases, sublaminate level scaling and ply-level scaling, the strength decreased as laminate thickness and hole diameter increased. By keeping the thickness constant and increasing the hole diameter, they found two different trends. For sublaminate level scaling, the strength decreased as hole diameter increased, whereas for specimens with clustering, the strength increased as hole diameter increased.

Since the stacking sequence, both at the ply-level and laminate level, modify the initiation and evolution of several damage mechanisms, it is relevant to analyze each damage mode in an isolated way. This fact can be studied, at least approximately, in some stacking sequences, such as cross-ply laminates [1].

To predict the global response of laminates containing holes, several methodologies, including analytical models such as the Whitney-Nuismer model, Continuum Damage Mechanics (CDM), and Stress Failure Criteria have been used [2-3,9-17]. In [18] a thorough review of constitutive models for damage on composites can be found. An alternative to these methodologies is the Discrete Damage Mechanics (DDM). DDM can predict the appearance of the first crack, evolution of crack density, and redistribution of stresses in the laminate due to degradation of mechanical properties of the cracked lamina. Among the models based on DDM ([1, 19-26]), [22] is selected in this work because of its balance of simplicity and accuracy.

Its simplicity is related to the fact that DDM is based on an analytical solution assuming periodicity and Griffith's criterion for fracture. It uses only two parameters, the critical energy release rates (ERR) in mode I and II (G_{IC}, G_{IIC}) to predict both initiation and evolution of matrix damage due to both shear and transverse stress. The fiber damage part of the model uses the longitudinal tensile strength of the lamina F_{1T} and the Weibull modulus m of the fiber. When used in finite element analysis (FEA), DDM is an inherently objective constitutive model, i.e., its response is independent of mesh density [27]. Although DDM's simplicity implies some limitations, it has been validated extensively with experimental data from many sources, for several materials and a multitude of laminate stacking sequences (LSS) [22, 28-35]. DDM has been able to predict crack density, as well as reduction of modulus, Poisson's ratio, and coefficient of thermal expansion (CTE) as a function of applied strain or stress, and crack density, quite accurately. It has also being able to predict the ultimate load of open-hole specimens [27, 33].

In this work, a study of the effect of ply-clustering in the matrix damage evolution is carried out. Several cross-ply stacking sequences with different cluster thicknesses and cluster locations are modeled. Crack density, applied load-displacement, and notched strength of the laminate are reported.

2. Numerical model

In this work the DDM model of Barbero-Cortes is used to analyze the evolution of matrix cracking. A detailed description of this model is included in [22] and [31]. A fiber damage model is added to estimate the transition to fiber failure that precedes ultimate fracture of the laminate and is described in [27] and [33]. The numerical model is implemented in Abaqus/Standard by programming a user subroutine UGENS (User General Section). In a previous work [33], the new formulation of the DDM model was extensively validated for laminates with and without holes, with several materials and configurations. Nine laminate lay-ups, with six different fibers (T300, T700, AS4, IM7, CCF300, and HTA) and nine matrices (1034C, 3502, 3501-6, APC2, 8552, 8911, 5228, 5428, and 6376-C), and seven plate geometries, were analyzed. Good correlation was found in both the failure load and the curve force-displacement.

A square plate of a x b = 15.24 x 15.24 mm^2 with an open centered circular hole of 3.18 mm diameter made from a carbon fiber reinforced epoxy laminate (T300/1034-C) was modelled, Fig.1. The plate is subjected to an in-plane tensile load applied in the direction of the 0^o plies. Laminates with several stacking sequences were analyzed. The mechanical properties of the material are taken from the literature [11, 14, 34] and are shown in Table 1.

The plate is discretized with a total of 2464 four-node shell elements (S4), as shown in Fig.1. The size of the elements is smaller close to the hole, to take into account the stress concentration. As it is demonstrated in an authors' previous work [27], the DDM model is mesh-independent. In that work, several mesh size were analyzed, and no influence of the mesh refinement on the global response and the crack-density evolution of the plate was observed.

The plate is fully assigned a low value of crack density (0.02 mm^{-1}) to seed the model for possible damage initiation. The load is applied in the horizontal direction by increasing

the displacement in opposite direction at the edges of the plate, Fig.1. No quarter-plate mesh is used to allow the future study of stacking sequences with orientations different to 0º and 90º. The vertical displacement on the nodes located at the lower corners of the plate is restricted.

3. Results

To analyze the influence of cluster thickness and its location several stacking sequences were selected; first each effect (thickness and location) is studied separately and then they are studied together. Crack-density evolution and longitudinal stress evolution as a function of applied strain are studied around the edge of the hole. Also, load-displacement/strain curves are reported. Additionally, contour plots of crack density and longitudinal stress are calculated for an applied load equal to the ultimate strength.

3.1. Influence of cluster thickness

To analyze the influence of the number of plies in a cluster (cluster thickness) the following pair of laminates has been studied. All of them contain 90º clusters with different numbers of plies located in the interior of the lay-up.

A: $[0_2/90_8]_S$ compared with $[0/90_4]_{2S}$

B: $[0_2/90_{10}]_S$ compared with $[0/90_5]_{2S}$

In both cases, laminates with the same number of plies at 0 ° and 90 ° but with different stacking sequences are compared. Interior 90º clusters with different numbers of plies exist on both types of laminates. The $[0_2/90_8]_S$ stacking sequence has a cluster of sixteen 90º plies, the $[0/90_4]_{2S}$ has a total of three 90º clusters, one of 8-plies (interior) and two of 4-plies (exteriors). The second pair of laminates has 20 plies at 90º. Whereas the $[0/90_4]_{2S}$ has two different clusters of 90º plies, one of 10 plies and two of 5, the $[0_2/90_{10}]_S$ has only one internal cluster of 20 plies.

It was observed that the behavior is similar for both pair of laminates (A and B), only the comparisons between $[0_2/90_{10}]_S$ and $[0/90_5]_{2S}$ laminates are reported in detail.

Crack-density evolution on 90º plies at the edge of the hole in all the laminates studied presents two different ranges as shown in Fig. 2a. First, crack density grows suddenly after crack initiation. After that, the curve displays a quasi-linear behavior until the applied load is close to the ultimate strength. Nevertheless, significant differences on the crack-density evolution, at the node situated at the edge of the hole, are observed between the three clusters. As the clustering of plies at 90º increases, damage starts at a lower applied displacement (as expected) and its growth rate is slower. Namely, the slope of the crack-density curve decreases as the clustering at 90º is thicker (slope of 20 plies at 90º > 10 plies at 90º > 5 plies at 90º). Also, from an applied strain of 0.25% (see top axis in Fig. 2a), the crack density for the thickest cluster is the lowest of the three clusters.

As far as the global response of the laminate is concerned, the applied force-displacement plot for both laminates is represented in Fig. 2b. For $[0/90_5]_{2S}$ laminate, the behavior is linear until failure. The laminate with a higher number of 90º plies in the cluster ($[0_2/90_{10}]_S$), has a reduction of slope for an applied strain of 0.3%. At laminate failure, the stiffness of the $[0/90_5]_{2S}$ laminate is slightly higher (4%) than the $[0_2/90_{10}]_S$ laminate. The ultimate strength of the $[0/90_5]$s is 8% higher than that of the $[0_2/90_{10}]_S$ laminate. Thus,

an increment in the number of plies inside the cluster reduces the ultimate strength. This is consistent with practical experience that indicates that thicker laminates are not desirable [36].

Therefore, the global stiffness and ultimate strength of laminates with the same number of plies but with different stacking sequences differs. In contrast, classical laminate theory (CLT) predicts that these values are the same for both studied laminates, since in CLT there is no dependence of stacking sequence on the in-plane behavior of a laminate. This result shows the importance of studying the clustering of plies with the same orientation.

The longitudinal stress on 0º plies is represented in Fig. 2c. Both laminates show the same behavior up to 0.1140% applied strain. From this point forward, the longitudinal stress in the $[0_2/90_{10}]_S$ laminate is higher than in the $[0/90_5]_{2S}$ laminate. In both cases, the maximum longitudinal stress is the fiber failure strength F_{1T}.

Contour plots are shown in Fig. 3 immediately before laminate failure. The loading direction is horizontal in the figure.

The crack density on the 90º plies is maximum at the edge of the hole (Fig.3a). The matrix damage is concentrated around this area and evolves perpendicular to the direction of the load application with a peanut shape. Little matrix damage in the 0º plies is observed for any applied load (Fig.3b).

The area where the maximum crack density on 90º plies is reached, is also the area where the longitudinal stress on 0º plies is maximum (Fig. 3c) due to stress re-distribution. When matrix damage grows, the stiffness decreases and a redistribution of the stress to the sides of the plate is produced. The lowest stress is found at the edge of the hole in the direction of the load application.

The longitudinal stress on 90º plies (Fig. 3d) grows perpendicular to the direction of the load application from the edge of the hole to the edge of the plate, and also around the edge of the plate in the direction of the load application. The maximum value of the stress is localized symmetrically at both sides of the edge of the hole in perpendicular direction to the load application (Fig. 3d).

As the number of 90º plies in the cluster decreases (from left to right), the peak crack-density value on 90º plies around the edge of the hole increases (Fig. 3a). However, its evolution is slower, as it is shown by smaller damage area.

For the $[0_2/90_{10}]_S$ laminate, as the cluster of 0º plies (2 plies) is thicker than for $[0/90_5]_{2S}$ laminate (1 ply), the crack-density evolution on 0º plies at the edge of the hole is more noticeable.

The contour plots of longitudinal stress on 0º plies are presented in Fig. 3c. In this case the differences between $[0_2/90_{10}]_S$ and $[0/90_5]_{2S}$ are minor.

In Fig. 3d, for the laminate with the larger cluster at 90º plies $[0_2/90_{10}]_S$ (left), the area with high longitudinal stress is smaller in extension and value (36.67 MPa) than for the $[0/90_5]_{2S}$ laminate (right), where it reaches 41.25 MPa.

3.2. Influence of cluster location

To analyze the influence of the cluster position, the following laminates were studied.

C: $[90_i/0]_{2S}$ for i =1,2…7

D: $[0/90_i/0]_{2S}$ for i =1,2…7

Both families of laminates (C and D) have the same orientations but different cluster location. For example, laminate $[90_7/0]_{2S}$ presents two external clusters of 7 plies at 90º on the surface, and two internals also with seven plies: [**90**$_7$/0/**90**$_7$/0$_2$/**90**$_7$/0/**90**$_7$]. On the other hand, laminate $[0/90_7/0]_{2S}$ presents four internal clusters of 7 plies at 90º: [0/**90**$_7$/0/**90**$_7$/0$_2$/**90**$_7$/0/**90**$_7$/0], two near the surface of the laminate (from now called external clusters) and two close to the center of the laminate (internal clusters).

It was observed that all laminates studied in this section display similar behavior. Therefore, only the results for $[90_7/0]_{2S}$ and $[0/90_7/0]_{2S}$ stacking sequences are shown in Figs. 4 and 5.

The crack-density evolution at the edge of the hole in each cluster of $[90_7/0]_{2S}$ laminate shows the same ranges as those described in Section 3.1: a threshold for the initial growth of the crack density followed by a quasi-linear region. Although the internal and external 90º clusters have the same numbers plies, the values of crack-density threshold and rate of crack-density growth are different. Therefore, for this laminate, cluster position is a determinant factor on crack-density evolution.

The threshold applied strain for crack initiation is lower (0.14%) for the external cluster than for the internal cluster (0.2%). The slope in the quasi-linear region of Fig. 4 is 39% lower for the external cluster than for the internal cluster.

Since all clusters in $[0/90_7/0]_{2S}$ are internal, they show the same behavior (Fig. 5), similar to that of the cluster in the $[90_7/0]_{2S}$ laminate. In this laminate, all clusters present the same behavior regardless of position. Therefore, the position of the cluster is relevant only if the cluster is located on the surface of the laminate

Contour plots are shown in Fig. 6 and 7 for the applied load that produces the maximum crack density in 90º plies, which corresponds to laminate failure.

The crack density on the 90º plies is maximum at the edge of the hole (Fig. 6a). Damage is concentrated around this area and evolves perpendicular to the load direction with a peanut shape. The load direction is horizontal in this figure.

The crack density contour plots shown in Fig. 7 are exactly the same for both internal and external cluster of $[0/90_7/0]_{2S}$ laminate. Incidentally, this explains the behavior shown in Fig. 5, with both, internal and external clusters behaving identically.

3.3. Coupled effect of thickness and position of the cluster

Three families (E, F, and G) of laminates are studied in this section. Each family has several pairs of laminates, each characterized by the number of plies "*i*" in the clusters.

E: $[0/90_i]_S$ compared with $[90_i/0]_S$ for i=1 to 7

F: $[0_i/90_i]_S$ compared with $[90_i/0_i]_S$ for i=1 to 4

G: $[0_2/90_i]_S$ compared with $[90_i/0_2]_S$ for i=2,8 and 10

Laminates with the same plies but inversely stacked were studied. Inverse stacking sequences have the same number of plies, orientations, and thicknesses, but mirrored ordering (for example, $[0/90_4]_S$ and $[90_4/0]_S$). In all pairs of laminates analyzed, one contains a cluster in the symmetry plane (internal cluster) with "2i" 90º plies, and the other has two clusters on the surface of the laminate (external clusters) that contains "i" 90º plies.

The evolution of crack density, applied load, and longitudinal stress with respect to the applied displacement (or applied strain), is identical for both laminates of each pair. This result can be explained as follows. The ERR of each case depends on two things: the thickness of the 90º cluster (composed of "i" plies) and whether the 90º cluster is located on the surface or not. Since a crack on the surface is not constrained (Fig. 8a), the ERR of a surface crack is the same as that of an interior crack with twice the thickness (Fig. 8b). For all cases, the center 90º cluster is twice as thick as the outside 90º cluster. Therefore, the behavior of each pair of laminates is identical.

Since all laminates display similar behavior, only the results for the $[0/90_4]_S$ stacking sequences and their inverse $[90_4/0]_S$ are shown in Fig. 9. The crack-density evolution in Fig.9 follows the same trends previously explained in Section 3.1.

When the 90º plies reach damage initiation (0.18% strain, Fig. 9a), load is transferred to the 0º plies, which can be seen as a change of slope in Fig. 9c (also at 0.18% strain). After that, the longitudinal stress on 0º plies grows until the fiber tensile strength is reached (1730 MPa), as shown in Fig. 9c.

The applied load-displacement curve of the $[0/90_4]_S$ laminate and its inverse stacking sequence are shown in Fig. 9b. A linear behavior until failure is observed. No significant change of laminate stiffness is observed due to the increment of damage. That is, laminate stiffness is dominated by the 0º plies. For this reason, it is virtually impossible to identify damage of carbon/epoxy laminates using experimental values of laminate stiffness vs. applied load or strain. The observed change is just too small for the precision of the instrumentation [37].

In Fig. 10, contour plots of crack density in 90º ply, and longitudinal stress in 0º and 90º plies are shown for an applied load where it is reached the ultimate strength (for a displacement of approx. 0.03 mm) for $[0/90_4]_S$. The same contour plots are observed for a laminate and its inverse stacking sequences; and the same behavior is found in all the cases studied. The contour plots for the longitudinal stress on 90º plies present the same shape and evolution as the one described in section 3.1.

4. Conclusions

In this work, several laminates with cluster of plies in different positions and different thicknesses are analyzed using the modified DDM model, which predicts damage localization and stress concentration. As expected, the maximum values of stresses are reached at the edge of the hole, perpendicular to the load direction. The lowest values are registered near the edge of the hole, along the centerline of the plate. The model predicts the behavior of surface cracks, cracks in constrained clusters, as well as the effect of cluster ply thickness.

Several differences are observed between laminates with the same number of plies but clustered differently. Laminates with higher number of 90º plies in a cluster yield lower ultimate strength. Additionally, damage starts for a lower applied load, and the extension of the damage area is larger.

Laminates with clusters of 90º plies with the same number of plies (same thickness) but in different position behave equally when the cluster is located in the interior of the laminate. The matrix cracking evolution is slower in clusters on the surface than clusters in the interior of the laminate, having both of them the same number of plies. Thus, cluster position is an important factor for crack-density evolution.

Laminates with inverse stacking sequences (in one of the laminates there is a cluster in the interior with double thickness and in the other laminate there is a cluster in the surface with half thickness), present no differences in terms of crack-density evolution, longitudinal stress evolution, applied load-displacement curve, and ultimate strength. This behavior is due to the relationship between the thicknesses and the position of the plies.

Acknowledgement

The authors are indebted for the financial support of this work to the Ministry of Economy and Finance of Spain (project DPI2013-42240-R).

References

[1] Swindeman MJ, Iarve EV, Brockman RA. Strength Prediction in Open Hole Composite Laminates by Using Discrete Damage Modeling. AIAA Journal 2013;51(4):936-45.

[2] Whitney JM, Nuismer RJ. Stress fracture criteria for laminated composites containing stress concentrations. Journal of Composite Materials 1974; 8: 253-65.

[3] Camanho PP, Maimı P, Davila CG. Prediction of size effects in notched laminates using continuum damage mechanics. Composites Science and Technology 2007; 67: 2715–27.

[4] Ercin GH, Camanho PP, Xavier J, Catalanotti G, Mahdi S, Linde P. Size effects on the tensile and compressive failure of notched composite laminates. Composite Structures 2013; 96:736-44.

[5] Lopes CS, Seresta O, Coquet Y, Gürdal Z, Camanho PP, Thuis B. Low-velocity impact damage on dispersed stacking sequence laminates. Part I: Experiments. Composites Science and Technology 2009; 69: 926–36.

[6] Harris CE, Morris DH. Role of delamination and damage development on the strength of thick notched laminates. In: Johnson, WS editor. Delamination and debonding of materials, ASTM STP 876, Philadelphia, 1985. p. 424–47.

[7] Vaidya RS, Klug JC, Sun CT. Effect of ply thickness on fracture of notched composite laminates. AIAA J 1998; 36(1):81–8.

[8] Green BG, Wisnom MR, Hallett SR. An experimental investigation into the tensile strength scaling of notched composites. Composites Part A: Applied Science 2007; 38: 867-78.
[9] Camanho PP, Erçin GH, Catalanotti G, Mahdi S, Linde P. A finite fracture mechanics model for the prediction of the open-hole strength of composite laminates. Composites Part A 2012; 43:1219-25.
[10] Kim JK, Kim DS, Takeda N. Notched strength and fracture criterion in fabric composite plates containing a circular hole. Journal of composite materials 1995; 29: 982-98.
[11] Tan SC. A progressive failure model for composite laminates containing openings. Journal of Composite Materials 1991; 25:556-77.
[12] Tsai KH, Hwan CL, Lin MJ, Huang YS. Finite Element Based Point Stress Criterion for Predicting the Notched Strengths of Composite Plates. Journal of Mechanics 2012;28(3): 401-6.
[13] Wang J, Callus PJ, Bannister MK. Experimental and numerical investigation of the tension and compression strength of un-notched and notched quasi-isotropic laminates. Composite Structures 2004; 64: 297-306.
[14] Maimí P, Camanho PP, Mayugo JA, Dávila CG. A continuum damage model for composite laminates: Part II – Computational implementation and validation. Mechanics of Materials 2007; 39: 909-19.
[15] Nuismer RJ, Whitney JM. Uniaxial failure of composite laminates containing stress concentrations. Fracture Mechanics of Composites, American Society for Testing and Materials 1975, 117-42.
[16] Van der Meer FP, Sluys LJ. Mesh-independent modeling of both distributed and discrete matrix cracking in interaction with delamination in composites. Engineering Fracture Mechanics 2010; 77:719–35.
[17] Van der Meer FP, Moës N, Sluys LJ A level set model for delamination – Modeling crack growth without cohesive zone or stress singularity. Engineering Fracture Mechanics 2012; 79:191–212.
[18] Dávila CG, Rose CA, Iarve EV. Modeling Fracture and Complex Crack Networks in Laminated Composites. In: Mantič V,editor. Computational and Experimental Methods in Structures: Volume 5. Mathematical Methods and Models in Composites, London, UK, Imperial College Press; 2013, 297-347.
[19] Awerbuch J., Madhukar M.S. “Notched strength of composite laminates: predictions and experiments – a review”. Journal Reinf Plast Comp. 1985, Vol. 4, pp. 3-159.
[20] Kortschot M.T., Beaumont P.W.R. “Damage mechanics of composite materials: I-measurements of damage and strength”. Composite Science and Technology. 1990, Vol. 39, pp. 289-301.
[21] Sheng Y, Yang D, Tan Y, Ye J. Microstructure effects on transverse cracking in composite laminae by DEM. Compos Sci Technol 2010;70:2093–101.

[22] Barbero EJ, Cortes DH. A mechanistic model for transverse damage initiation, evolution, and stiffness reduction in laminated composites. Composites Part B 2010;41:124-32.
[23] Biscaia HC, Micaelo R, Teixeira J, Chastre C. Numerical analysis of FRP anchorage zones with variable width. Composites Part B 2014; 67:410–26.
[24] Sadeghi G, Hosseini-Toudeshky H, Mohammadi B. In-plane progressive matrix cracking analysis of symmetric cross-ply laminates with holes. Fatigue and Fracture of Engineering Materials and Structure 2014; 37: 290-305.
[25] Sadeghi G, Hosseini-Toudeshky H. Experimental damage evolution and failure mechanisms in GFRP composite laminates with open holes. In: Bi-Annual international conference on experimental solid mechanics and dynamics (X-Mech-2014), Tehran, Iran, February, 2014.
[26] Maheo L, Dau F, André D, Charles JL, Iordanoff I. A promising way to model cracks in composite using Discrete Element Method. Composites: Part B 2015; 71: 193-202.
[27] Moure MM, Sanchez-Saez S, Barbero E, Barbero EJ. Analysis of damage localization in composite laminates using a discrete damage model. Composites Part B 2014; 66: 224-32.
[28] Cortes DH, Barbero EJ. Stiffness reduction and fracture evolution of oblique matrix cracks in composite laminates. Annals of Solid and Structural Mechanics 2010; 1(1): 29-40.
[29] Barbero EJ, Cosso FA. Determination of Material Parameters for Discrete Damage Mechanics Analysis of Carbon-Epoxy Laminates. Composites Part B 2014; 56: 638--46.
[30] Barbero EJ, Cosso FA. Benchmark Solution for Degradation of Elastic Properties due to Transverse Matrix Cracking in Laminated Composites. Composite Structures 2013; 98: 242-52.
[31] Barbero EJ, Cosso FA, Martinez X. Identification of Fracture Toughness for Discrete Damage Mechanics Analysis of Glass-Epoxy Laminates. Applied Composite Materials 2014; 21(4):633-51.
[32] Barbero EJ, Sgambitterra G, Adumitroaie A, Martinez X. A Discrete Constitutive Model for Transverse and Shear Damage of Symmetric Laminates with Arbitrary Stacking Sequence. Composite Structures 2011; 93:1021-30.
[33] Moure MM, Otero F, García-Castillo SK, Sánchez-Sáez S, Barbero E, Barbero EJ. Damage evolution in open-hole laminated composite plates subjected to in-plane loads. Composite Structures 2015; 133: 1048-1057
[34] Camanho PP, Dávila CG, Pinho ST, Iannucci L, Robinson P. Prediction of in situ strengths and matrix cracking in composites under transverse tension and in-plane shear. Composite: Part A 2006; 37:165-76.
[35] M. Ghayour, H Hosseini-Toudeshky, M. Jalalvand, and E. J. Barbero, Micro/macro approach for prediction of matrix cracking evolution in laminated composites, Journal of Composite Materials, 0(0):1–13, 2015.

[36] Pierron F, Green B, Wisnom MR. Full-field assessment of the damage process of laminated. Composite open-hole tensile specimens. Part I: Methodology. Composites: Part A 2007; 38: 2307-20.
[37] Barbero EJ, Cosso FA, Roman R, Weadon TL. Determination of material parameters for Abaqus progressive damage analysis of E-Glass Epoxy laminates. Composites Part B: Engineering 2013; 46:211-220.

Figures

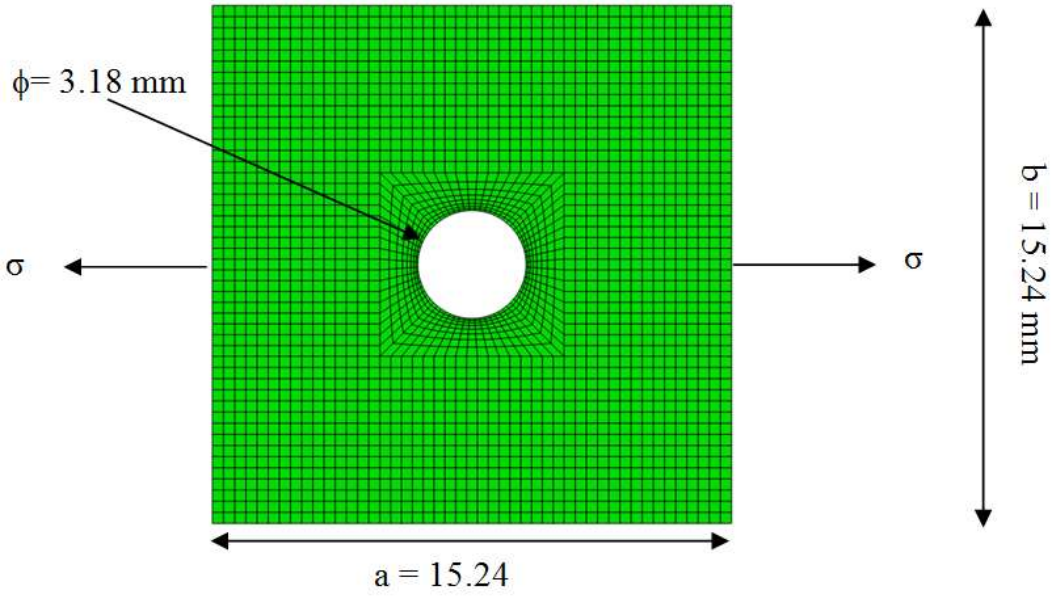

Fig. 1. Mesh and geometry configuration used in the simulations.

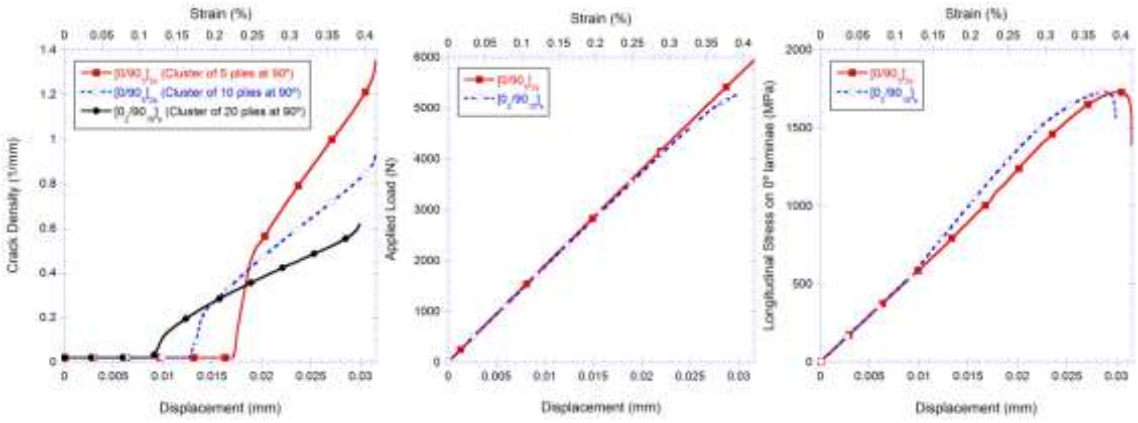

(a) (b) (c)

Fig. 2. Comparison of $[0/90_5]_{2s}$ and $[0_2/90_{10}]_s$ laminates: a) crack-density evolution on 90º plies in the node situated at the edge of the hole for three different clusters of 90º plies, b) Applied-load evolution and c) Longitudinal stress on 0º plies in the element situated above the edge of the hole.

(a)

(b)

(c)

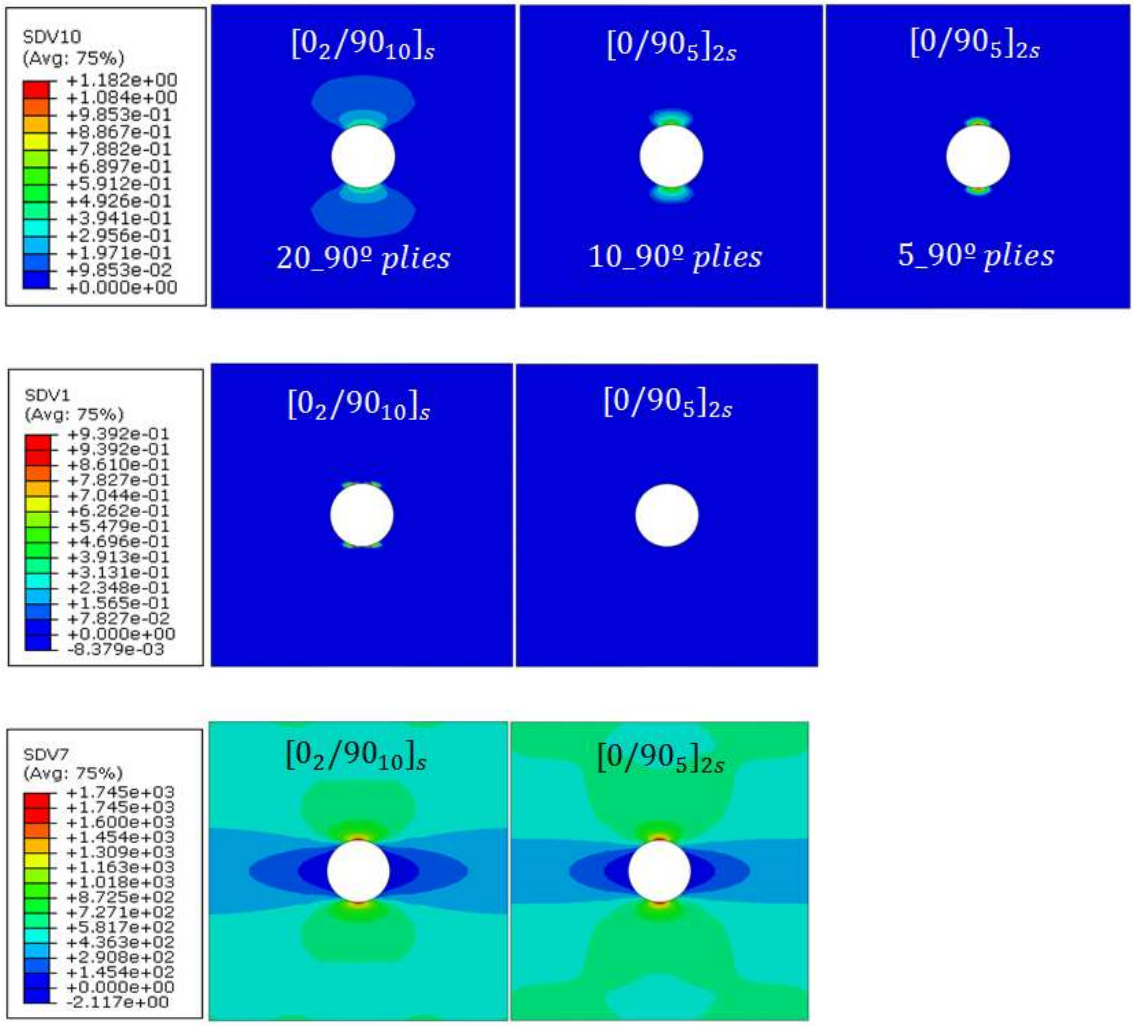

Fig. 3. Comparison between $[0_2/90_{10}]_s$and $[90_5/0]_{2s}$ laminates. a) From left to right: 20, 10, and 5 ply, 90º clusters. Crack-density evolution on 90º plies, b) From left to right: 2 and 1 ply, 0º cluster. Crack-density evolution on 0º plies, c) Longitudinal stress on 0º plies and, d) Longitudinal stress on 90º plies.

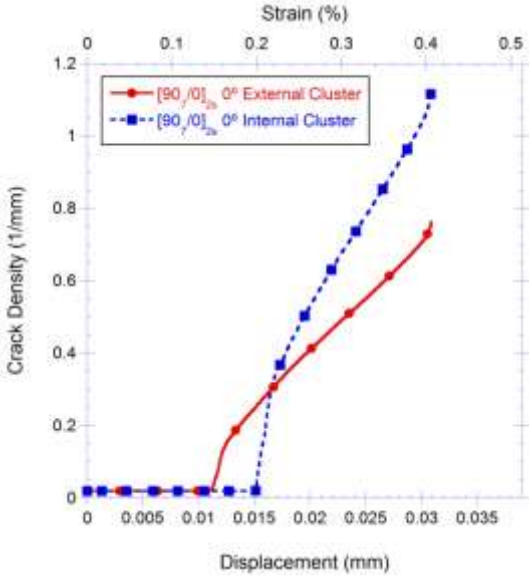

Fig. 4. Crack-density evolution on 90º plies in the node situated at the edge of the hole, for $[90_7/0]_{2s}$ laminate

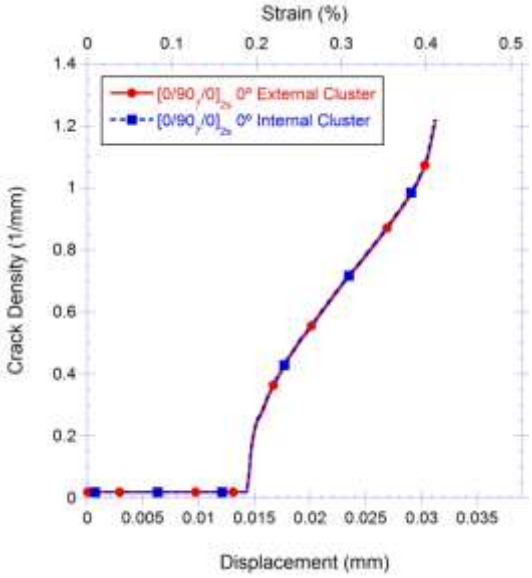

Fig. 5. Crack-density evolution on 90º plies in the node situated at the edge of the hole, for $[0/90_7/0]_{2s}$ laminate

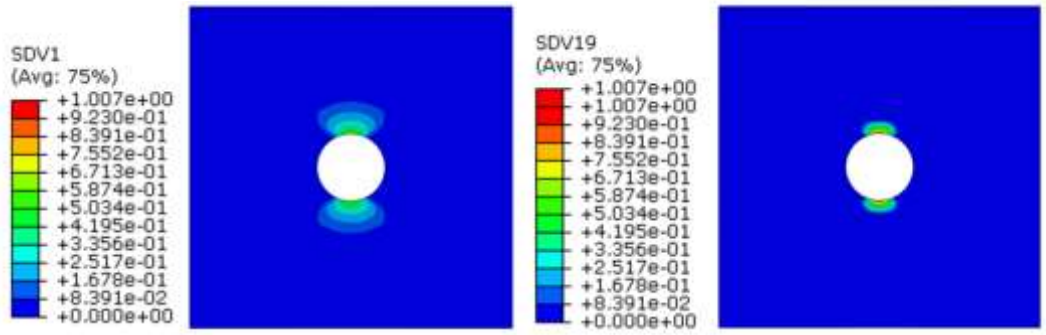

(a) (b)

Fig. 6. Crack-density evolution in $[90_7/0]_{2s}$ laminate. a) 90º external cluster, b) 90º internal cluster.

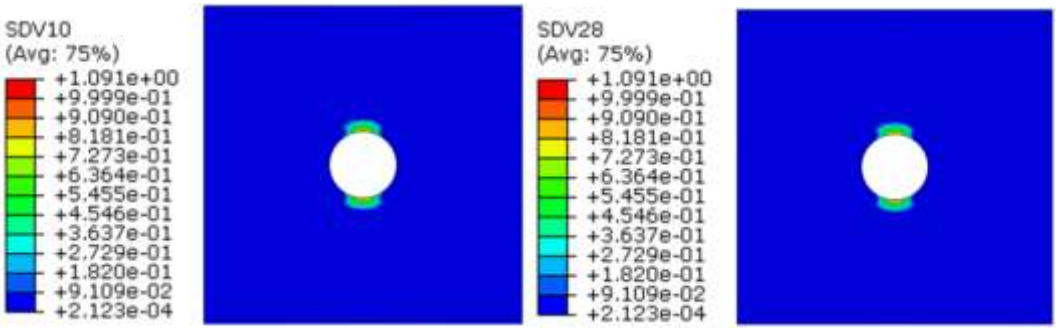

(a) (b)

Fig. 7. Crack-density evolution in $[0/90_7/0]_{2s}$ laminate. a) 90º external cluster, b) 90º internal cluster.

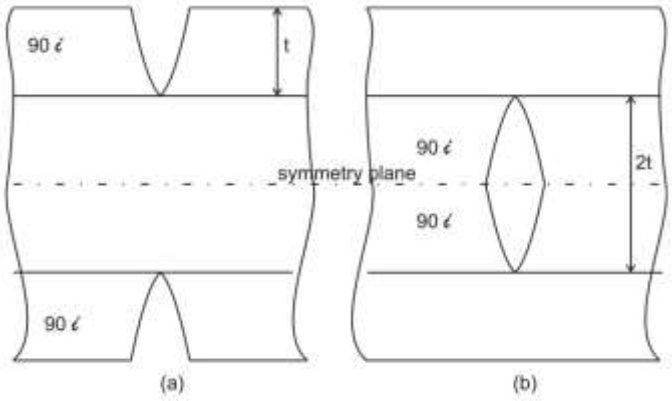

Fig. 8. Inverse laminates: a) crack in a surface 90º cluster, and b) crack in an interior 90º cluster.

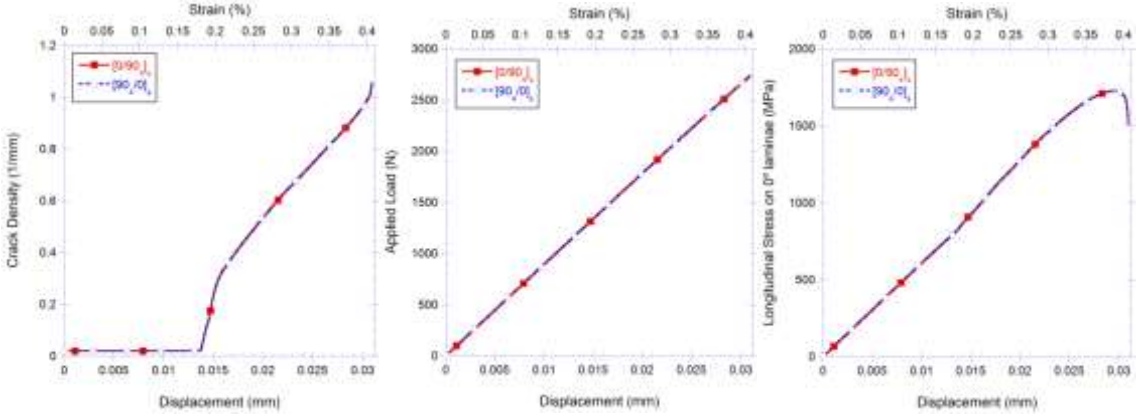

(a) (b) (c)

Fig. 9. a) Crack-density evolution on 90º plies in the node situated at the edge of the hole, b) Applied-load evolution of the laminate and c) Longitudinal stress on 0º plies in the element situated above the edge of the hole, for $[0/90_4]_s$ vs $[90_4/0]_s$, laminates.

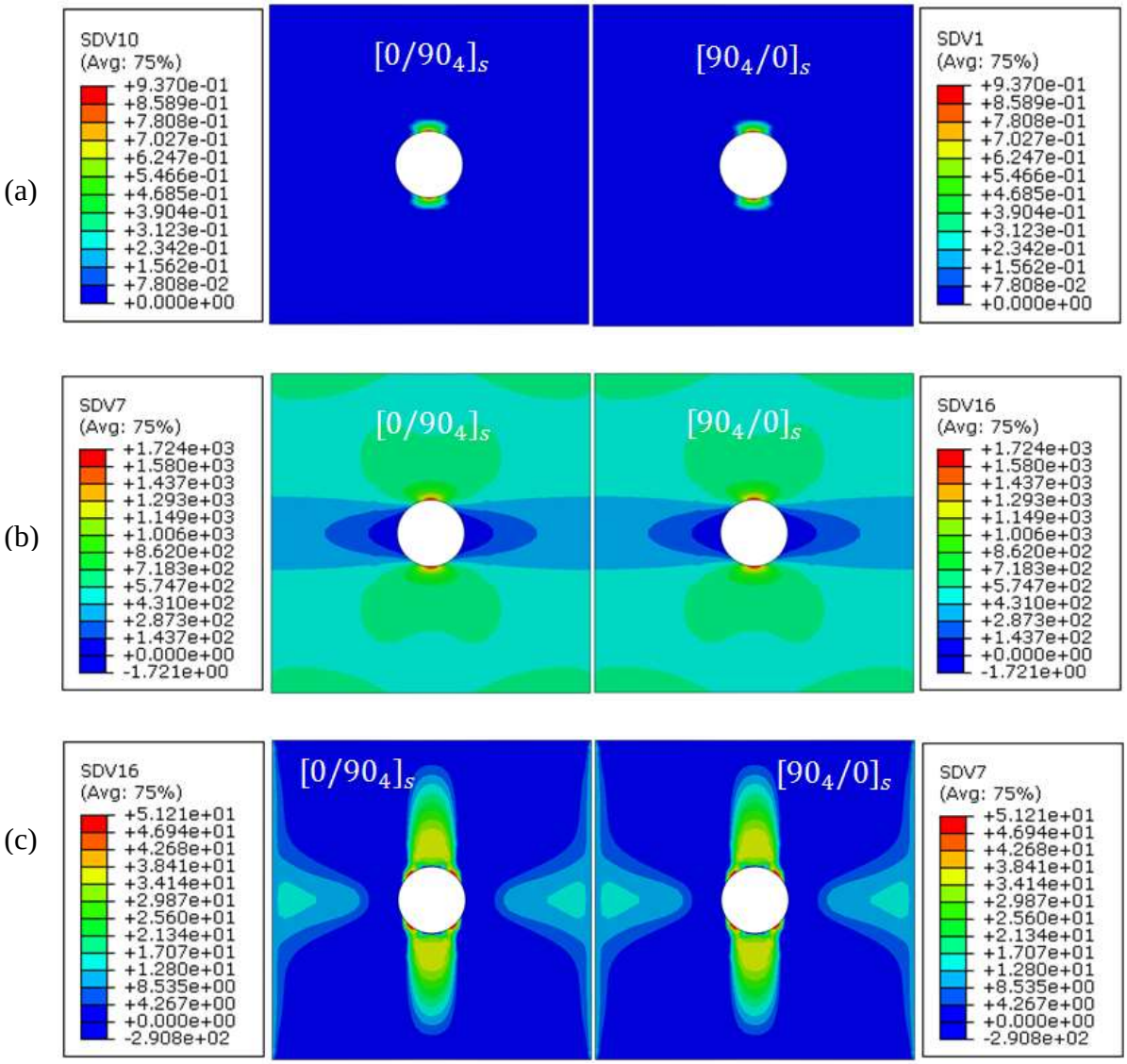

Fig. 10. Comparison between $[0/90_4]_s$ and $[90_4/0]_s$ laminates. a) Crack-density evolution on 90º plies b) Longitudinal stress on 0º plies and c) Longitudinal stress on 90º plies.

Tables

Property	Units	Value
Strain release rate in mode I G_I	$[kJ/m^2]$	0.228
Strain release rate in mode II G_{II}	$[kJ/m^2]$	0.455
Tensile failure strength in the fiber direction F_{1t}	$[MPa]$	1730
Compressive failure strength in the fiber direction F_{1c}	$[MPa]$	1379
Tensile failure strength in transversal direction F_{2t}	$[MPa]$	66.5
Compressive failure strength in transversal direction F_{2c}	$[MPa]$	268.2
Shear failure strength F_6	$[MPa]$	58.7
Transition thickness t_t	$[mm]$	0.8
Weibull modulus m	-	3
Young modulus in the fiber direction E_1	$[MPa]$	146800
Young modulus in transverse direction E_2	$[MPa]$	11400
In-plane shear modulus G_{12}	$[MPa]$	6100
In-plane Poisson ratio ν_{12}	-	0.3
Out-of-plane Poisson ratio ν_{23}	-	0.42
Lamina thickness t_k	$[mm]$	0.1308

Table 1. Mechanical properties of T300/1034-C [11, 14, 32].